Forest Ecology and Management 595 (2025) 122989

Contents lists available at ScienceDirect

Forest Ecology and Management

journal homepage: www.elsevier.com/locate/foreco

Precision forestry in actively managed loblolly pine plantations: Leaf area index response one growing season following a variable-rate fertilization

Chris W. Cohrs [a], Al Lyons [b], Timothy J. Albaugh [c], David R. Carter [c], Otávio C. Campoe [d], Rafael A. Rubilar [e,f], Matthew Sumnall [c], Andrew Trlica [a,*], Mark V. Corrao [g], Simerjeet Virk [h], Rex Lester [i], Rachel L. Cook [a]

[a] Department of Forestry and Environmental Resources, North Carolina State University, Raleigh, NC 27695-8008, USA
[b] Southern Operations Forest Management, Manulife Investment Management, Harpersville, AL 35078, USA
[c] Virginia Tech Department of Forest Resources and Environmental Conservation, 228 Cheatham Hall, Blacksburg, VA 24061, USA
[d] Federal University of Lavras, Lavras, Mato Grosso, Brazil
[e] Cooperativa de Productividad Forestal y Laboratorio de Investigación en Suelos, Aguas y Bosques (LISAB), Departamento de Silvicultura, Facultad de Ciencias Forestales, Universidad de Concepción, Victoria 631, Casilla, Concepción 160-C, Chile
[f] Centro Nacional de Excelencia para la Industria de la Madera (CENAMAD) – ANID BASAL FB210015, Pontificia Universidad Católica de Chile, Santiago, Chile
[g] Department of Forest, Rangeland, and Fire Sciences, College of Natural Resources, University of Idaho, Moscow, ID 83844, USA
[h] Department of Crop and Soil Sciences, University of Georgia, Tifton, GA 31793, USA
[i] Lesco Aviation Group, 6370 Shenandoah Lane, Olive Branch, MS 38654, USA

A R T I C L E I N F O

Keywords:
Loblolly pine
Leaf area index
Variable-rate fertilization
Sentinel-2
Precision silviculture

A B S T R A C T

Forest management at a sub-stand level will be a critical part of optimizing future productivity gains for timber or carbon objectives. We developed a methodology to apply "precision forestry" on one-hectare grids in operational loblolly pine (*Pinus taeda* L.) plantations in east Texas to quantify responses to site-specific nutrient management and vegetation control based on measures of leaf area index (LAI). First, we cross-validated satellite-derived (Sentinel-2) LAI with airborne laser scanning (ALS)-derived LAI and found the strongest linear relationship with the Above and Below Ratio Index (ABRI) method ($R^2 = 0.83$). Five post-thin midrotation stands, totaling 256 ha, were divided one year prior to fertilization with one part receiving herbicide treatment for competition control. Fertilization was applied in a grid pattern via fixed-wing aircraft with rates (0 to or 336 kg N ha^{-1} + 33.6 kg P ha^{-1}) determined based either on LAI derived from satellite imagery or randomly assigned. We fit a linear mixed effect model (conditional $R^2 = 0.83$) to predict the change in seasonal peak LAI from pre-fertilization (October 2020) to one growing season post-fertilization (October 2021). Main effects of LAI-based vs. random application, average understory height, N rate applied, and herbicide application status were all significant ($p < 0.05$). Increases in LAI were greater where fertilizer rates were based on remotely sensed LAI prior to application as compared to randomly assigned rates. Increases in LAI also correlated to increases in fertilizer application rate. Areas with understory vegetation below 3 m in height exhibited greater increases in LAI following fertilization. The effects of fertilizer can persist for multiple years, thus the long-term impacts of variable-rate fertilization in operational pine plantations, and in combination with vegetation control, will require additional time to assess the return on investment for these management practices. This study demonstrates the feasibility and potential efficiency gains available by informing treatment planning at a sub-stand scale with remotely sensed canopy metrics.

* Corresponding author.
E-mail addresses: cohrs.xyz@gmail.com (C.W. Cohrs), allyons416@hotmail.com (A. Lyons), tim_albaugh@vt.edu (T.J. Albaugh), carte134@msu.edu (D.R. Carter), otavio.campoe@ufla.br (O.C. Campoe), rafaelrubilar@udec.cl (R.A. Rubilar), msumnall@vt.edu (M. Sumnall), altrlica@ncsu.edu (A. Trlica), mcorrao@uidaho.edu (M.V. Corrao), svirk@uga.edu (S. Virk), rexalester@me.com (R. Lester), rlcook@ncsu.edu (R.L. Cook).

https://doi.org/10.1016/j.foreco.2025.122989
Received 7 March 2025; Received in revised form 1 June 2025; Accepted 8 July 2025
Available online 24 July 2025

1. Introduction

Forest plantations currently supply around one-third of the world's industrial roundwood, an amount that could increase to one-half of the global supply by 2030 if intensive silvicultural practices are widely implemented (Fox et al., 2011). The US forest products industry has one of its major centers of activity in the southeastern US (SEUS) (Alig and Butler, 2004) which is largely dependent on loblolly pine- (*Pinus taeda* L.) based planted and managed systems (Wade et al., 2019). This SEUS region produces 61 % of the nation's industrial roundwood and is the largest single producer in the world, supplying approximately 16 % of global demand (Guo et al., 2023; Wear and Greis, 2002) on approximately 16.8 million hectares of softwood plantations (Oswalt et al., 2019). The high productivity of loblolly plantations is due in large part to advancements made in silviculture over the last 70 years that have increased average regional productivity from 3–4 m^3 ha^{-1} yr^{-1} in the 1950s to 9–12 m^3 ha^{-1} yr^{-1} of stem volume over a 25-year rotation (Fox et al., 2007). Supply pressure for forest products is expected to increase along with decreases in available forestland, thus requiring even higher rates of productivity on less total land area (Payn et al., 2015).

Because soil nutrient deficiencies of nitrogen (N) and phosphorous (P) are very common in the SEUS (Fox et al., 2007), the addition of fertilizer is often a necessary silvicultural practice both at the time of planting and midrotation. Allen (2001) concluded that nutrient additions were needed on most sites within the SEUS to achieve optimum rates of production. Fertilization with N and P has demonstrated a significant growth response in many N and P deficient soils (Albaugh et al., 2019; Pritchett and Swinford, 1961; Gent et al., 1986), averaging an additional 3.5 m^3 ha^{-1} yr^{-1} over eight years from one application of 224 kg ha^{-1} N and 28 kg ha^{-1} P (Fox et al., 2007). The majority of southern pine plantations are thought to potentially benefit from N and P supplementation by the crown closure stage (Fox et al., 2007). Still, the number of pine plantations being fertilized annually has steadily declined over the past two decades in response to several adverse economic shifts, with most recent estimates of only about 240,000 ha compared to a historical peak of approximately 640,000 ha fertilized in 1999 (Albaugh et al., 2019).

Based on the recommendations of Fox et al. (2007), the SEUS forest industry currently "blanket" applies fertilizer at equal rates across stands typically between 12 and 80 ha in size, one to three times during a 25-year rotation, usually applied as 426 kg ha^{-1} urea and 140 kg ha^{-1} diammonium phosphate (DAP; Albaugh et al., 2019). Response to fertilization can be quite variable, from 0.5–10 m^3 ha^{-1} yr^{-1} (Albaugh et al., 2012), due in part to the fact that nutrient availability is influenced by soil chemical, physical, and biological characteristics, and remains one of the least understood aspects of forest science (Bahr et al., 2013; Subedi et al., 2015).

This inherent variability in nutrient limitation is common within most agricultural fields and presents comparable challenges for crop management through uniform applications of nutrients. Therefore, among different site-specific management strategies commonly utilized in precision agriculture today, variable-rate application of fertilizer to address this within-field nutrient spatial variability is a widely adopted practice in row-crop farming systems (Lowenberg-DeBoer and Erickson, 2019). The demonstrated benefits of site-specific nutrient management in row crops including improved nutrient management and crop yields (Srinivasan, 2006), making this approach a promising nutrient management practice worthy of investigation for implementation across other major industries, including forestry in the SEUS.

Fertilization—particularly with N—has been shown to lead to increased leaf area index (LAI), a ratio quantifying the projected leaf surface area per unit of ground area (Vose et al., 1988). For intensively managed loblolly pine, LAI serves as an indicator of nutrient status and potential future volume growth (Allen et al., 2001). Higher LAIs correspond with a greater capacity to intercept light, photosynthesize, and fix carbon (Will et al., 2005). Historically, LAI values below 3.5 have suggested fertilization, weed control, or other silvicultural interventions were needed (Allen, 2001). Typically, LAI is measured as a stand approaches midrotation, nearing and entering canopy closure and the stem exclusion stage of stand development. Levels of LAI are commonly assessed as an indicator of stand productivity and the need for nutrient additions to improve production and harvest yields. In addition, the interaction between chemical release treatments (*i.e.,* herbicide application to competing understory) and fertilization at midrotation has been explored, indicating additive benefits to volume growth when herbicide and fertilizer were paired together (Albaugh et al., 2012). Previous research has shown that competing vegetation density estimated via passive multispectral sensors was inversely related to crop tree LAI, but only deciduous competition was considered (Blinn et al., 2012). However, response in LAI to fertilization with- and without understory control has yet to be explored, particularly in evergreen understory environments.

A critical technological advancement in the forestry industry has been the use of data products from remote sensing systems such as passive multispectral satellites and light detection and ranging (LiDAR), which enable one to indirectly monitor many biophysical tree- and stand-level metrics of forest productivity, such as LAI. Forest management companies have been incorporating the use of remote sensing imagery from orbital satellites or airborne LiDAR instruments (ALS) to assess the LAI of their stands throughout a rotation. In passive satellite remote sensing, LAI has most commonly been estimated as a function some specific spectral vegetation index (SVI), a linear combination of multiple spectral bands intended to respond to a surface physical trait of interest (Franklin et al., 1997). Bottom-of-atmosphere reflectance values, which are processed to account for atmospheric distortion between the satellite sensor and the ground, are often used in these applications to analyze forest canopy characteristics. In contrast, measurement of LAI in the field, including via potentially inconsistent "ocular estimates", is often laborious and may show less distinct relationships with stand and site factors than remotely sensed indicators like vegetation indices (Peduzzi et al., 2010).

Most recently, LAI of loblolly pine in the SEUS was estimated using multispectral imagery acquired via Sentinel-2, a passive remote sensing constellation comprised of two satellites operated by the European Space Agency (ESA), at a 10-meter spatial resolution with an accuracy of 0.4 units of LAI, modeled with satellite reflectance metrics to a goodness-of-fit R^2 of 0.81 (Cohrs et al., 2020). Loblolly pine LAI has also been estimated using ALS-derived point return metrics with an R^2 of 0.90 and a standard error of 0.35 units of LAI (Sumnall et al., 2016). While LiDAR can be more expensive to acquire than satellite data, one of many additional benefits afforded by LiDAR is its capacity to yield more detailed measurements of forest structure, such as the capacity for separate estimate of LAI in evergreen understory and evergreen forest canopy, which unlike deciduous understory species cannot be readily differentiated by satellite data (Blinn et al., 2012; Sumnall et al., 2021).

To confidently prescribe rates of fertilizer based on remotely sensed LAI, it is important to determine margins of error involved in the models for predicting LAI from remotely sensed data and to assess the way LAI responds to fertilizer rates based on the initial state of pine canopy LAI and competing understory conditions. Further, if the competing understory is evergreen, the extent to which passive multispectral sensors can successfully gauge changes in canopy LAI is of interest for forest management practitioners without access to bespoke LiDAR datasets.

The goal of this study was to evaluate the feasibility of using passive and active remote sensing to estimate stand canopy and understory LAI, use this information as a guide for variable-rate fertilizer application of managed loblolly pine stands (both with and without competing vegetation control), and evaluate the potential for using LAI as a tool for monitoring site response to management. Specifically, our objectives were to: 1) Construct and test a system for delineating managed loblolly pine plantations for variable-rate fertilization based on LAI; 2) Evaluate remote sensing tools for detecting LAI change and examine LAI response

after one growing season post-fertilization and vegetation control; and 3) Compare LAI response and changes in stand-level variation due to LAI-based variable-rate fertilizer application vs randomly selected fertilizer rates ranging from 0 to 336 kg N ha^{-1} + 10 % P by mass.

2. Methods

2.1. Site descriptions and stand histories

Five stands, totaling 256 ha, were selected for establishing a variable-rate fertilization regime both with and without herbicide treatment near Woodville, TX. Stands varied in total area (Fig. 1), though were all at midrotation stage (ages ranged 14–22 at time of fertilization) and had been recently thinned to similar densities (300–500 tree ha^{-1}) and basal areas (15–23 m^2 ha^{-1}) (Table 1).

Soils ranged from clayey to coarse loamy and well drained to poorly drained, with differences in estimated depth to an argillic subsoil horizon, underlying geologic parent material and other notable diagnostics between stand boundaries (Table 2).

All five stands were manually split approximately in half using ArcGIS Pro v2.2.4 (ESRI, Redlands, CA) for herbicide applications in such a way as to be operationally feasible regarding roads and access constraints. Further care was taken so underlying soils were not confounded with herbicide treatments, when possible. Herbicide was applied to the target areas via skidder application in May 2020 (Table 3). Understory species were primarily the evergreen, and included shrub yaupon (*Ilex vomitoria* A.), as well as blackberry (*Rubus* spp.) and devil's walking stick (*Aralia spinosa* L.). The tank mix for all stands was 1419 ml Isopropylamine salt of Imazapyr, 710 ml 83.9 % triclopyr butoxyethyl ester, 30 ml 60 % Metsulfuron methyl, 118 ml Elite Velocity drift control agent, and 946 ml Elite Supreme surfactant at a rate of 281 L ha^{-1}.

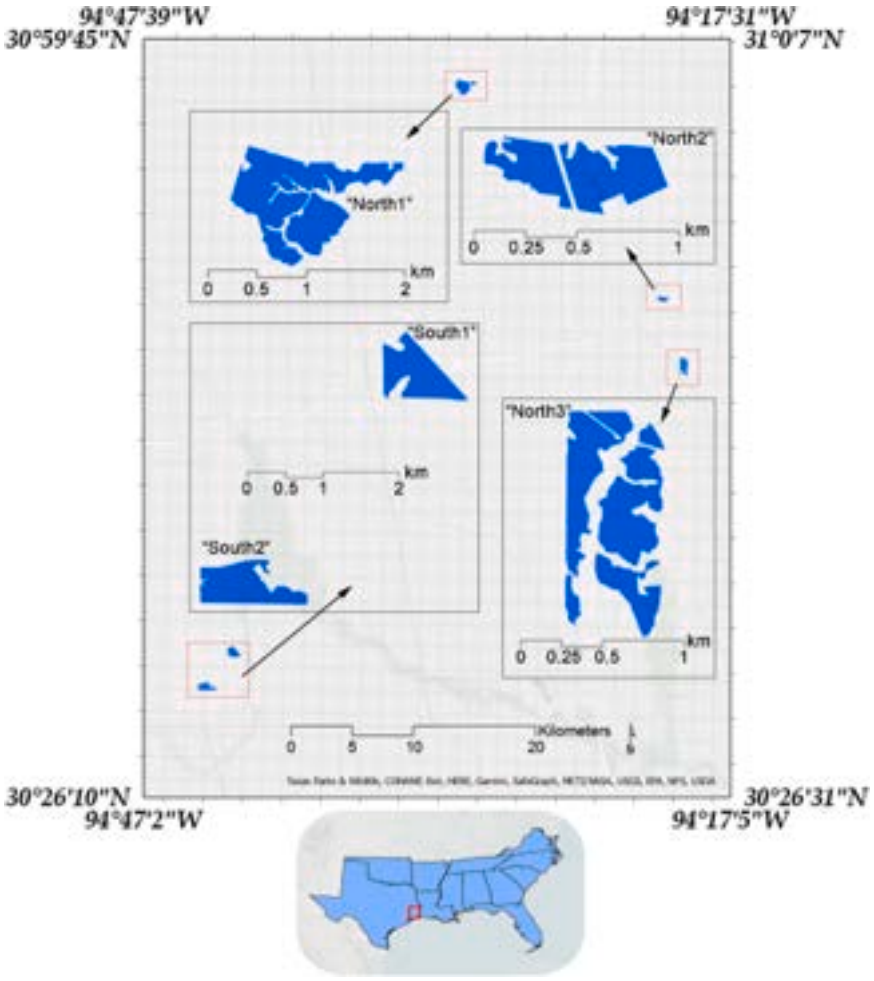

Fig. 1. Location map of five stands in eastern Texas where a variable-rate fertilization × vegetation control study was established.

Table 1
Stand history prior to herbicide application and variable-rate fertilization. Also shown: Basal Area (BA) and quadratic mean diameter (QMD).

Stand ID	*Date Planted*	*Date Thinned*	*Density (trees ha^{-1})*	*BA (m^2 ha^{-1})*	*QMD (cm)*	*Total Stand Area (ha)*
North1	2004	Apr 2019	524	16	19.6	87.4
North2	2004	Nov 2019	494	16	20.3	17.8
North3	2007	Sep 2019	467	15	20.3	47.8
South1	2004	Apr 2019	469	16	20.6	51.0
South2	1999	Jan 2020	356	23	28.7	52.2

Table 2
Summary of primary soils for the five stands in our variable-rate fertilization study near the Woodville, TX area.

Stand ID	*Dominant profile texture*	*Depth to argillic subsoil*	*Drainage*	*Underlying geology*	*Other features*
North1	Clayey	0–12.5 cm	Moderately well drained	Claibourne group	Mixed clays; root limited profile
North2	Clayey	12.5–25 cm	Moderately well drained	Willis formation	Mixed clays; root limited profile
North3	Fine Loamy	50–100 cm	Well drained	Willis formation	Siliceous; root limited profile
South1	Coarse Loamy	25–50 cm	Well drained	Lissie formation	Eroded surface; siliceous
South2	Coarse Loamy	None within 200 cm	Poorly drained	Lissie formation	Silty surface; Alfic subsoil; natric

Table 3
Summary of herbicide application for the five stands in our variable-rate fertilization study near the Woodville, TX area.

Stand ID	*Date of Treatment*	*Area Treated (ha)*	*Total Stand Area (ha)*
North1	19 May 2020	33.6	87.4
North2	19 May 2020	6.1	17.8
North3	20 May 2020	16.2	47.8
South1	11 May 2020	16.2	51.0
South2	12 May 2020	22.7	52.2

2.2. Remote sensing and auxiliary data for retrieving leaf area index

2.2.1. Retrieving pre-fertilization LAI for variable rate planning using Sentinel-2 data

To estimate LAI prior to fertilization in spring 2021, two Level-2A (atmospherically corrected/bottom-of-atmosphere surface reflectance) Sentinel-2 image granules were downloaded from the Copernicus dataspace browser (Copernicus Data Space Ecoystem, 2020), both with acquisition dates of 30 September 2020. The two southern stands (South1 and South2) shared one image granule and the three northern stands (North1, North2, North3) shared a separate single image granule. Cloud cover (including shadows), snow and ice, and other potentially image-degrading features were quantified via metadata filtering and spectral profiling of individual plots. Total cloud coverage percentages were 21.0 % for the image shared by the southern stands and 4.0 % across the entire granule, with 0.0 % cloud coverage shrouding any stand boundaries. Images were snow/ice free and no pixels were flagged with degraded quality. Stand boundaries were inspected for roads, logging decks, and other non-canopy features based on visual inspection of true color (RGB) band composite Sentinel-2 imagery. Such undesired features were then clipped from a vector boundary created from the original stand boundaries, within which canopy LAI was calculated via the Sentinel-2 rasters.

LAI was calculated using the following equation (Cohrs et al., 2020):

$$\boldsymbol{LAI} = 0.310 \times \boldsymbol{SR} - 0.098 \quad (1)$$

where ***SR*** is the Simple Ratio, a SVI calculated as the ratio of the near-infrared (842 nm) and red (665 nm) bands (Band 8 and Band 4, respectively) using Sentinel-2 Level-2A surface reflectance. Sentinel-2 imagery taken after herbicide application was used to plan the LAI-based fertilizer applications (see 2.3). Large reductions in LAI were noted in many areas applied with herbicide due to reduction in green competing understory vegetation (Fig. 5), which resulted in many of the LAI-based treatment grids in the herbicide areas receiving fertilizer rates at the higher end of the scale (Table 4). Fertilizer rates in the LAI-based treatment grids were assigned irrespective of the potential influence of understory vegetation, rather than attempting to adjust rates based on a blanket factor to correct for the unquantified loss of understory vegetation that might vary considerably within and between stands. Fertilizer rates in the Random and Control prescription categories were assigned without reference to LAI in areas both applied and not applied with herbicide, ensuring that all levels of fertilizer rate/herbicide/prescription type were replicated adequately.

2.2.2. Retrieving monthly LAI using Sentinel-2 data

Retrieval of LAI based on Sentinel-2 imagery was also performed on a monthly mean basis starting in the pre-trial period through thinning, herbicide and fertilizer application, and up to nine months post-fertilization (December 2018–January 2022) via a slightly different approach. Using Google Earth Engine (Gorelick et al., 2017), three raster stacks were produced each covering one or more stands, with 38 rasters in each stack corresponding to monthly average LAI (calculated with Eq. 1). Each stack element was constructed based on individual Sentinel-2 Level-2A scenes with < 90 % total cloud coverage selected from all scenes overlapping the minimum bounding box of the five study stands. Those scenes were then cloud-masked using the *s2cloudless* cloud probability data product (Zupanc, 2019) with a cloud probability threshold of > 20 % and near-infrared cutoff for shadow detection of < 0.15. Normalized difference snow index (NDSI; Salomonson and Appel, 2004) was calculated for every scene, after which pixels with NDSI > 0.8 were also masked. After pixel masking and cropping to the minimum bounding box of the study stands, only imagery with > 70 % clear unmasked pixels was further retained use in producing mean monthly composite gridded LAI estimates. We believed that using monthly LAI averages calculated from multiple quality-checked scenes rather than LAI derived from single acquisitions would produce more accurate estimations of canopy LAI on a temporal scale. Further, the combined raster stacks enabled time series analysis of the stands prior to multiple major silvicultural events other than the variable-rate fertilization (e.g., thinning and herbicide application).

2.2.3. Comparing LAI estimated using ALS and Sentinel-2

We acquired ALS data during January 2021 collected via a Riegl 1560ii LiDAR (RIEGL, Horn, Austria) sensor at an average of 20 pulses m^{-2} attached to a fixed-wing aircraft. All pre-processing and LAI calculation tasks were implemented as described in Sumnall et al. (2021). Three different approaches were used to calculate pine canopy LAI: one using the Above and Below Ratio Index (ABRI), and two implementations using the Beer-Lambert Law methodology. The two Beer-Lambert methods differed in that model coefficients for over- and understory were either derived separately (Beer-Lambert$_1$), or by

Table 4
LAI was acquired from Sentinel-2 on 30 Sept 2020 (post-herbicide) and used for assignment of "LAI-based" fertilizer treatments the following schedule. All phosphorus (P) rates were 10 % of nitrogen (N) rates.

		Leaf area index (estimated via Sentinel-2)					
		1.0 – 1.5	**1.5 – 2.0**	**2.0 – 2.5**	**2.5 – 3.0**	**3.0 – 3.5**	**> 3.5**
Fertilizer Rate (kg ha^{-1})	N	336	280	224	168	112	none
	P	33.6	28	22.4	16.8	11.2	

combining under- and overstory LAI (Beer-Lambert$_2$) when creating the model. Predictions of LAI from all three ALS-based models were incorporated as rasterized grids at 15 m spatial resolution. These ALS-based LAI estimates were compared with LAI estimates based on Sentinel-2 simple ratio (SR) in virtue of the demonstrated strong relationship between this vegetation index and ground-measured LAI in managed loblolly pine stands (Cohrs et al., 2020).

2.3. Delineation of stands into variable-rate fertilizer treatments

Within stand boundaries a 100 × 100 m management grid was imposed, intended to match the spread patterns and accuracy estimates for the variable-rate fertilizer application equipment on the aircraft. An external 100 × 100 m dataset—the US National Grid (USNG) for Region VI, Texas UTM 15—was clipped to each stand boundary and each grid was given a unique identifier to serve as treatment plots. Interior square plots of 40 × 40 m were then created within each treatment grid to serve as "remote-sensing measurement plots" if they met quality criteria (*i.e.,* no logging decks, streams, or roads). The size of these measurement plots was based on a desired approximate number of trees per plot needed to form a representative subsample, and including a minimum 30 m buffer from adjacent treatments.

Because of the irregular shapes of forest stands, grids with an area less than 0.4 ha were *a priori* given neighboring prescription rates (assigned in a clockwise directional pattern beginning in north orientation, see Fig. 2) and were not considered in the study plot randomization and prescription allocation process. These "neighbor" assignments were made to reduce operational challenges during fertilizer application.

After the 100 × 100 m treatment grids were delineated, the weighted mean LAI for each gridded section of the stand (after manual exclusion of logging decks, roads and non-target species from stand boundary) was then calculated (Eq. (1)) based on LAI estimated in the post-thin, post-herbicide application imagery from 30 September 2020, and stored for each respective 100 × 100 m grid (occurs between (b) and (c) in Fig. 3). Next, each treatment grid was randomly assigned for fertilizer application as either 1) **LAI-based**; 2) **Control** (0 kg N ha^{-1} + 0 kg P ha^{-1}), or 3) **Random,** corresponding to a random assignment of either 112 kg N ha^{-1} + 11.2 kg P ha^{-1}, 224 kg N ha^{-1} + 22.4 kg P ha^{-1}, or 336 kg N ha^{-1} + 33.6 kg P ha^{-1}. The LAI-based approach assumes that, all other factors equal, lower LAI is indicative of lower nutrient supply and greater need for nutrient supplementation (Fox et al., 2007). Fertilizer rates are then assigned to supply additional N and P to grid cells with lower LAI (Table 4). Factors for prescription type were randomly assigned and stratified so that there was roughly an even number of replications for each combination of prescription type (Control, LAI-based, Random) and N fertilizer level both the herbicide-applied and non-applied portion of each stand. In total there were 412 treatment grids and 133 remote-sensing measurement plots (40 × 40 m interior square grids).

Treatments were assigned across stands with attention to the number of observations at each treatment level so as not to bias results (Fig. 6). As such, "control" treatments coinciding with zero fertilizer were counted within the "random" category. LAI-based rates were applied in increments of 56 kg N ha^{-1} to more closely track differences in LAI between grid cells, while Random rates were applied in increments of 112 kg N ha^{-1}, leading to an uneven distribution of as-applied fertilizer rates that created unbalanced replication. To create uniformity across as-applied fertilizer rate distributions, for analysis the fertilizer rates were grouped and treated as a fixed effect in our final model: 0, 112 (low), 168 + 224 (medium), and 280 + 336 (high) kg N ha^{-1}. A total of 216 treatment blocks greater than 4047 m^2 in area were installed (Table 5).

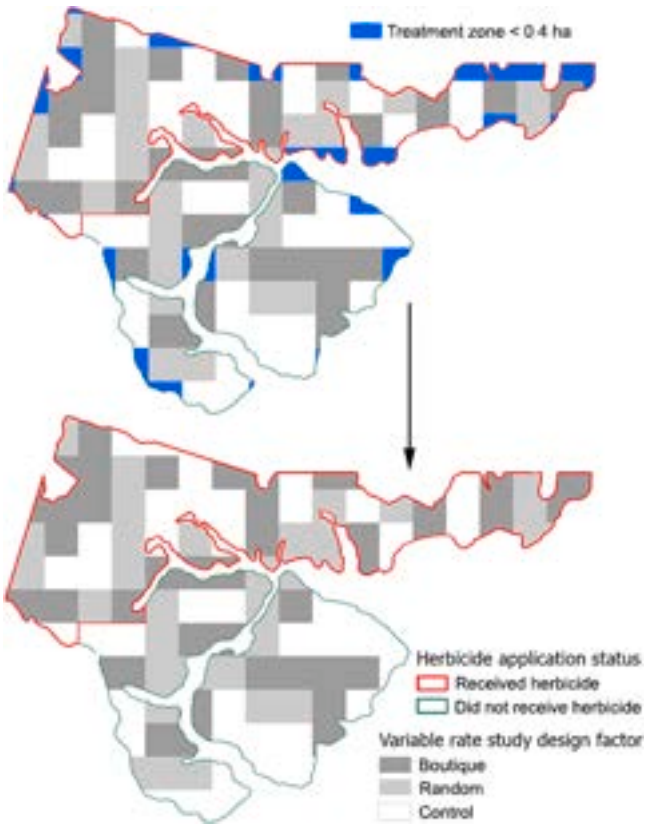

Fig. 2. Assignment of external variable-rate fertilization treatment zones to small grid areas (<0.4 ha, blue) which get their rates assigned based on neighboring cells of sufficient size.

2.4. Field data collection

A total of 77 permanent field plots were established pre-fertilization (December 2020) and re-measured one growing season post-fertilization (December 2021). Field plots were distributed across the full spatial extents of all stands and stratified by treatments (Fig. 4). The average plot area was approximately 300 m^2 with approximately 16 trees per plot. Understory estimates were obtained for each plot extent, recording total percentage of ground cover occupied by understory with living foliage, and fraction of total percentage understory that was evergreen or deciduous. Maximum and mean understory heights were also measured via vertex hypsometer. A Garmin GPSMAP 64sx global positioning system (GPS) receiver was used to record the coordinates of the corners of all field plots and the bases of trees where height and HTLC was measured.

2.5. Variable-rate fertilizer application flight

Variable-rate fertilizer application was performed on the 26th of March, 2021, following a calibration flight conducted on the 20th of March, 2021 at Inverness, MS. Both operations were conducted via the same Air Tractor AT-802A/N8058L, a fixed-wing aircraft with a maximum shaft horsepower of 1295 at 1700 RPM and a hopper capacity of 3028 L. The gate controlling dry fertilizer granules release was operated via a field computer (touch screen console) located in the cockpit, with an electric-over-hydraulic (EOH) cylinder attached to the gate box door that measured a constant rate of voltage, which in turn regulated the gate setting for each respective application rate (all aircraft undergo swath pattern testing). The standard 2.54 cm manual gate box was replaced with a Transland 25.4 cm gate box. Each control cylinder was set upon installation to open in increments ranging from a numerical value of 0 (closed) to 100 (fully open). Fertilizer was distributed via a high-volume gravity-fed Transland 10-vane

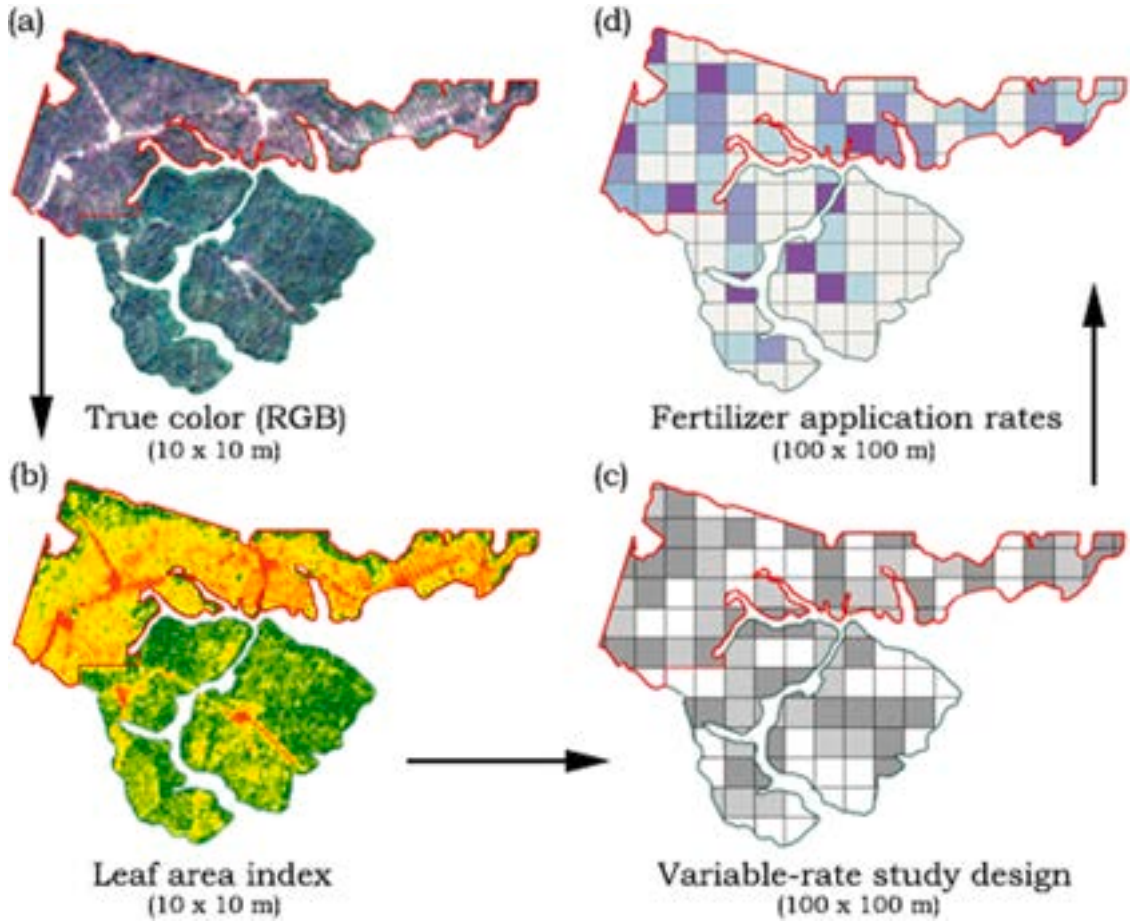

Fig. 3. Generalized flow diagram for constructing a variable-rate fertilization study design. Shown are (a) true color imagery using the red, green, and blue (RGB) 10 m bands of Sentinel-2, post-herbicide application (designated via red outline); (b) Sentinel-2-derived LAI calculated using Eq. (1), post-herbicide; (c) Delineation of variable-rate study design treatment grids (dark gray = LAI-based, light gray = Random, white = Control; (d) Fertilizer application rates, classified per study design factor as either 1) LAI-based (Table 4), 2) Control (0 kg N ha^{-1} + 0 kg P ha^{-1}), or 3) Random assignment of either 112 kg N ha^{-1} + 11.2 kg P ha^{-1}, 224 kg N ha^{-1} + 22.4 kg P ha^{-1}, or 336 kg N ha^{-1} + 33.6 kg P ha^{-1}. Weighted mean LAI calculated within each grid using plot boundaries quality-controlled to exclude roads, logging decks, and other non-forested areas. Values in parentheses are spatial resolutions for each data level.

Table 5
Summary of number of treatment blocks with area > 4047 m^2 installed across all five stands in this study. Blank entries indicate treatment combinations not tested.

Fertilizer N rate (kg N ha^{-1})	LAI-Based		Random/Control		Total
	Herb.	No Herb.	Herb.	No Herb.	
0	1	26	37	26	90
112	13	15	11	15	54
168	10	9	–	–	19
224	5	1	6	–	12
280	11	1	–	11	23
336	–	–	16	2	18
Total	40	52	70	54	216

(adjustable) spreader operating via Venturi distribution (forward aperture opening 25.4 cm × 96.5 cm). Equipped on the aircraft was a Satloc G4 GPS console set to constantly log position. The gate controller was a pre-programmable Vonduran Hydromax electric-over-hydraulic cylinder electrically actuated from the cockpit controls.

Prior to the flight, the desired swath width, bulk density, and application rates were entered into the controller software alongside the variable-rate fertilizer prescription GIS data, enabling fertilizer rate changes corresponding to targeted rates within plots. Controller software output, including GPS location relative to the fertilizer prescription map, was directly linked with the mechanism that opened and closed the feeder gate. Real-time metadata related to the flight and controller were matched with the GPS flight path and logged throughout the operation (*e.g.*, product density, application rate (amount per hectare), airspeed, gate box opening (gate settings), and swath width). A narrower swath (24.4 m) was used than is operationally standard to assure uniformity by letting the controller software increase or reduce the gate opening in correspondence with varying fertilizer rates. Prescribed N and P rates were converted from elemental rates to urea and DAP, taking into account N added through DAP (Table 6). Urea and DAP were applied in separate passes of the aircraft.

For the initial calibration flight, urea was applied at rates in the following order: 112, 224, 168, 280, 336, and 112 (kg N ha^{-1}) in grids roughly 0.40 ha in size (management zones for the experiment were 1 ha each). The swath width for calibration was also set to the same width to be used in the experimental application (24.4 m). In each application rate zone, eleven catch pans (31.75 × 19.05 cm) were arranged linearly approximately 2.4 m apart inside the treatment plots across the application plane flight path to evaluate the cross-track spread of fertilizer and determine the applied rate versus the controller gate settings using Cgoldenwall (1/1000 g) scales. After the calibration flight concluded, the spreader vanes were adjusted and tightened to their corrected settings and kept static for the operational application.

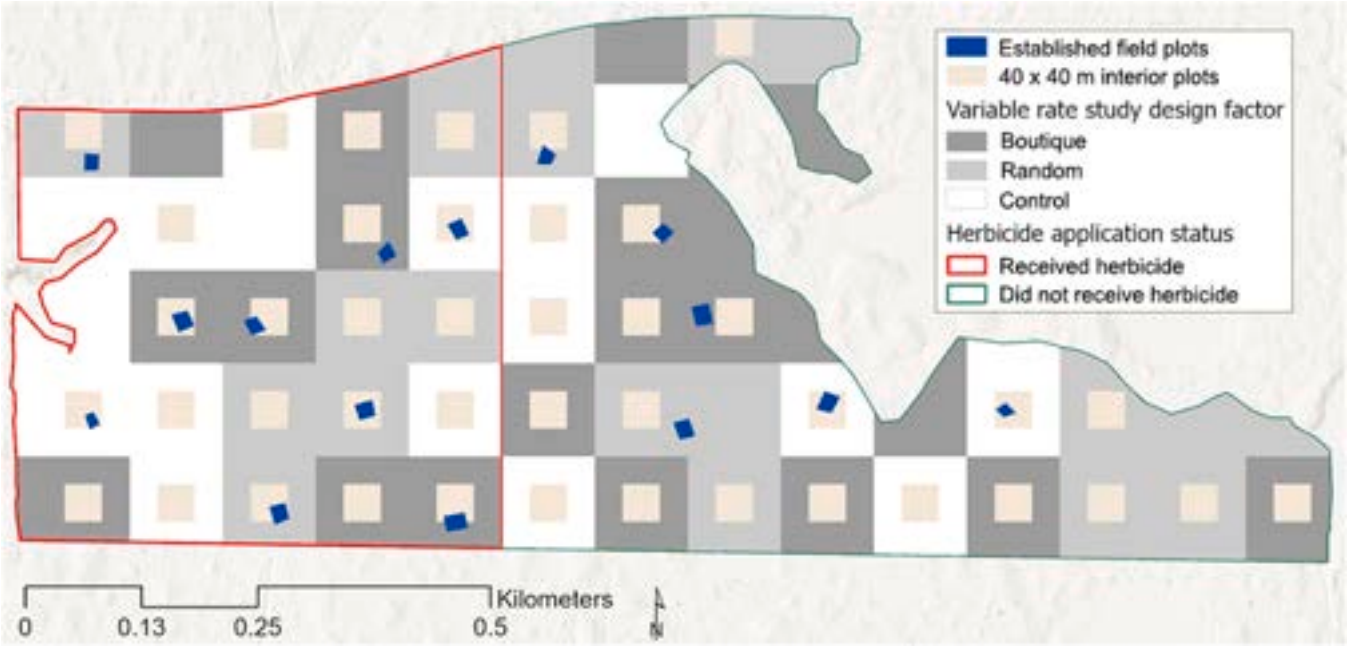

Fig. 4. Map of "South2", one of five stands showing remote-sensing measurement plots (40 × 40 m plots), and field plots (blue squares), herbicide application boundary splits (red outline = herbicide), and fertilization application method (i.e., variable rate study design factor) in shades of gray and white.

Table 6
Standardized rates of diammonium phosphate (DAP) and urea as applied to the treatment plots. Values in bold were used in both Random and LAI-based treatments, while non-bold were used only in LAI-based treatments.

Prescribed rate of elemental N	*Prescribed rate of elemental P*	*DAP as-applied (kg ha^{-1})*	*Urea as-applied (kg ha^{-1})*
0	0	0	0
112	**11.2**	**56**	**222**
168	16.8	84	332
224	**22.4**	**112**	**444**
280	28	140	554
336	**33.6**	**168**	**665**

2.6. Statistical analysis

Comparisons between Sentinel-2-based and ALS estimates of canopy LAI were made using simple linear regression, whereby estimates for each of the three ALS models were individually regressed against Sentinel-2-based estimates. Individual LAI estimates (observations) were calculated for all 133 interior 40 × 40 m measurement plots based on the downloaded 30 September 2020 Sentinel-2 imagery, and on the LAI estimates derived from the coincident ALS flights. The JMP application v15.2 (SAS Institute Inc., Cary, NC) was used to evaluate these relationships.

We also explored the evolution of LAI for each stand prior to and following treatment applications. We combined pixel-mean LAI estimated from the monthly Sentinel-2 imagery over the 133 observations from the remote-sensing measurement plots (40 × 40 m central grids) with field measurements taken from 73 overlapping field measurement plots ($n = 73$). A linear mixed-effect model was used to assess LAI response to factors of fertilization treatment. Our dependent variable, LAI change, was calculated as the difference between October 2021 LAI and October 2020 LAI as these periods represent seasonal peak LAI occurring both immediately prior to and after fertilizer applications. Our model fit random intercepts for herbicide treatment (herbicide/no herbicide) nested within stands as these were equivalent of spatially contiguous plots within which gridded treatments were assigned. Fixed effects were estimated for fertilizer variable rate factor ("LAI-based" or "Random"), average understory height (based on post-treatment mean average height falling above or below the pre-treatment mean of approximately 3 m, i.e. "3 m and below" and "above 3 m"), herbicide application factor (either received an herbicide application or did not), and nitrogen rate applied (categorized into four groups: "0", "112", "168 + 224", and "280 + 336", to match the more limited number of random N levels assigned (see 2.3). Specific interactive effects were examined based on hypothesized effects on pine canopy and the ability to achieve model conversion, including interactions between variable rate factor and average understory height, variable rate factor and herbicide control, variable rate factor and N rate applied, and N rate applied with herbicide control.

The final formula was:

$$\Delta LAI_{Oct20\text{–}Oct21} = VR + H_u + Herb + N + (VR \bullet H_u) + (VR \bullet Herb) + (VR \bullet N) + (N \bullet Herb)$$

where $\Delta LAI_{Oct20\text{–}Oct21}$ is the change in monthly mean LAI from October 2020 to October 2021, VR is variable rate factor, H_u is the understory height category, $Herb$ is the herbicide treatment category, N is the N rate category, and interaction effects are shown in parentheses.

We performed the relevant tests to assess the assumptions of normality of residuals, normality of random effects, linearity of relationships between fitted values and residuals, and homogeneity of variance. Multicollinearity was checked using Pearson correlation coefficient, with slight collinearity occurring between variable rate factor and N rate applied ($r < 0.5$). All mixed-model analysis was performed using R v 4.2.0 (R Core Team, 2022), using packages *lme4* (Bates et al., 2015), *performance* (Lüdecke et al., 2021), *emmeans* (Lenth, 2025), and

Table 7
Summary of variable-rate fertilization calibration flight conducted just prior to operational-setting variable-rate application.

Target rates (kg ha^{-1})		*112*	*224*	*168*	*280*	*336*	*112*
***Actual rates** (kg ha^{-1})*	*Mean*	125	225	172	283	339	126
	Std. Dev	15	19	14	27	40	13
	CV (%)	14	10	9	11	13	11
	% of Target Rate	112 %	100 %	102 %	101 %	101 %	113 %

Table 8
Summary of variable-rate fertilization by total urea and DAP applied per stand (stands fertilized 26 March 2021).

Stand ID	*Hectares Treated*	*Total Stand Area (ha)*	*Urea applied (tonnes)*	*DAP applied (tonnes)*
North1	44.1	87.4	17.2	4.3
North2	11.0	17.8	5.4	1.4
North3	27.1	47.8	12.1	3.0
South1	34.2	51.0	15.5	3.9
South2	27.4	52.2	9.9	2.5
		TOTAL	60.1	15.1

multcomp (Hothorn et al., 2008). We performed simultaneous comparisons across treatment factors based on the estimated marginal means of the fitted mixed model, applying Sidak's correction to the confidence intervals of the means to control for a family-wise error rate of $\alpha = 0.05$. In reporting our results, we utilized the following levels of evidence respective to p-values: very strong evidence ($p < 0.001$), strong evidence (p 0.001–0.01) some or moderate evidence (p 0.01–0.05), or weak evidence (p 0.05–0.10) (Muff et al., 2022).

3. Results

3.1. Variable-rate application, calibration and operational flights

The calibration flight showed high accuracy compared to programmed target rates (Table 7; Appendix A), with a good match between targeted and actual rates in variable rate fertilizer application by fixed wing aircraft. Post-variable-rate fertilizer application summaries for total area treated and the amount of urea and DAP applied were recorded for all five stands (Table 8)).

3.2. Results of comparing Sentinel-2 to ALS for estimated canopy LAI

There were strong linear relationships exhibited for all three ALS-based LAI sensing methods versus the Sentinel-2-based approach, with the ABRI method showing the best fit ($R^2 = 0.83$, Fig. 7c), followed by the two Beer-Lambert Law methods (Fig. 7a and b).

3.3. Analysis of remotely sensed LAI response

Time series of LAI in the different measurement plots showed considerable diversity in starting LAI and LAI trends that appear to be responsive to stand treatments (Fig. 5). Individual experimental units (treatment grids) were distributed somewhat evenly across different

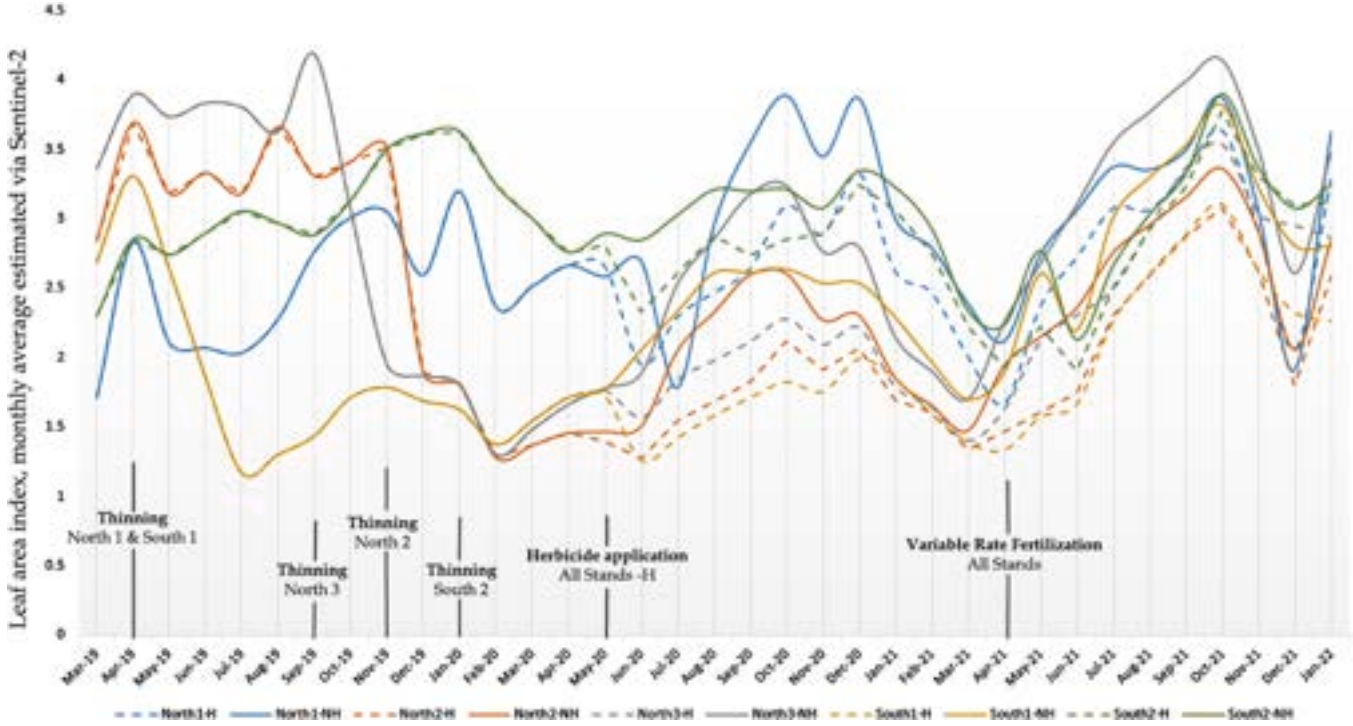

Fig. 5. LAI time series for all stands in which a variable-rate fertilization with midrotation herbicide release study was conducted (pixel means from all 40 × 40 m central grid cells). Five original stands were split approximately in half for this study, in which midrotation release treatment via herbicide took place in May 2020. LAI trajectories overlap prior to herbicide application and stand split, after which those five original stands are considered ten separate stands. Herbicide (H, solid) and no herbicide (NH, dashed) lines overlap in stands prior to treatment application.

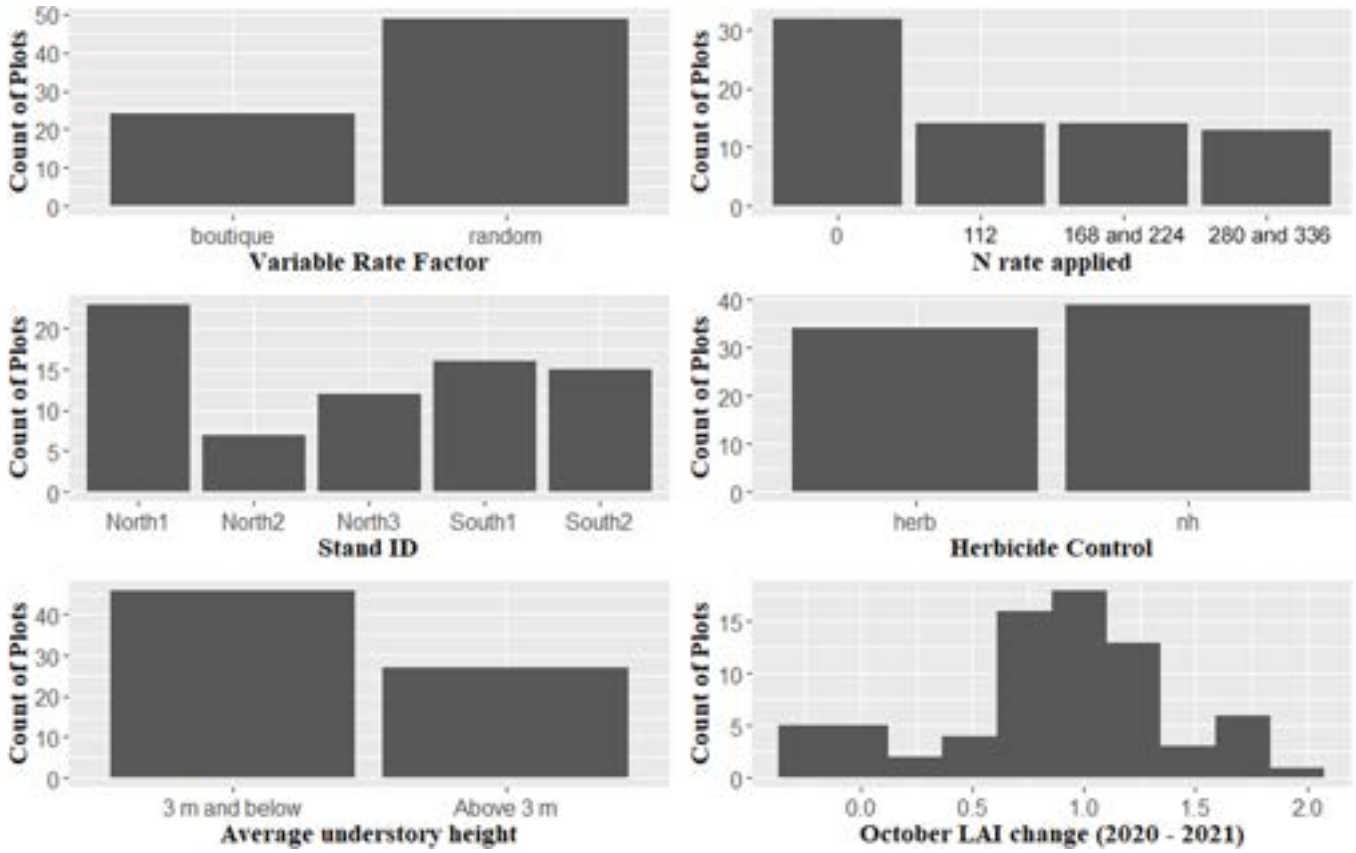

Fig. 6. Histograms of variables used in models reported in the variable-rate fertilization study. Total number of plots = 73. N rate applied is in units of kg N ha^{-1}. "Control" fertilizer levels were counted with "Random" for analysis. For herbicide control, "herb" and "nh" stand for received herbicide and did not receive herbicide, respectively.

treatment factors and covariates except for larger numbers of 0 fertilizer rate plots due to the contribution of both the Control prescription types and the occurrence of 0 rate in high-LAI grid cells (Fig. 6). LAI change was distributed nearly normally, with a mean annual change of around 1.0 LAI units. The linear mixed effect model to predict the change in Sentinal-2 derived LAI from pre-fertilization (October 2020) to one growing season post-fertilization (October 2021) had substantial explanatory power (conditional R^2 0.84; marginal R^2 0.33). Type III ANOVA showed very strong to strong evidence for the main effects of variable rate factor (either LAI-based or Random), average understory height, N rate applied, and herbicide application (Table 9).

Comparison of means showed changes in LAI were greater in Random applications, where understory was 3 m and below, and where N rates were above 0 (Fig. 8). Positive LAI gains were noted even in 0 N rate plots likely due to ongoing recovery of canopy foliage in the remaining crop trees after thinning. There was a weak general trend of greater LAI gain with greater rates of N across all the 40 × 40 m measurement plots (Pearson's ρ 0.42, $p < 0.001$), and all plots with supplemental N + P saw higher LAI gains (Fig. 9). Within any level of N, LAI-based and random prescriptions were statistically similar, though the narrower distributions in the LAI-based blocks suggest that the stand response in LAI was more variable when fertilizer rates were assigned with no respect to starting LAI values. We saw strong evidence for an interaction between variable rate factor and average understory height. LAI gain in LAI-based fertilizer treatments with shorter understory (< 3 m height) somewhat outperformed LAI-based treatments with taller understory (> 3 m height), while there was no difference in Random treatments (Fig. 10). All N treatment levels > 0 kg ha^{-1} were statistically indistinguishable from treatments with the highest LAI gains, in both LAI-based and Random prescriptions.

Effects of herbicide treatment varied somewhat by stand. Mean LAI change ranged from up to almost a 1.3 unit increase in the herbicide treatment areas down to essentially zero in the no herbicide treatment of one stand (Table 10), but LAI gains were higher in treatments that had been previously treated with herbicide compared to neighboring no-Herbicide stands.

Change in mean October LAI was generally higher in areas first treated with herbicide, but varied within stands at small spatial scales (Fig. 11). The greater LAI response in the herbicide-applied areas may have been due to both 1) higher fertilizer rates in the subpopulation of grid cells with LAI-based fertilizer rates, and 2) possibly greater LAI gain in the canopy trees due to diminished competition for additional nutrients from understory vegetation. This two-way interaction between amount of fertilizer nutrients added versus the LAI response in the stand is illustrated in Fig. 12, showing the example of stand "South1". High change in LAI was often but not always accompanied by high fertilizer application rates, illustrating the potential to achieve additional efficiencies in fertilizer applications in intensive pine plantations of this kind.

4. Discussion

4.1. Comparing LAI estimated using ALS and Sentinel-2

We found the strongest linear correlations between Sentinel-2 LAI estimated via the SR index (Cohrs et al., 2020) and ALS remote sensing products for estimating canopy LAI using the ABRI method (Sumnall et al., 2016, 2021). For this application, we assume a strong correlation also exists between ALS-derived estimates of LAI and more traditional ground-based measurement techniques reliant on light extinction

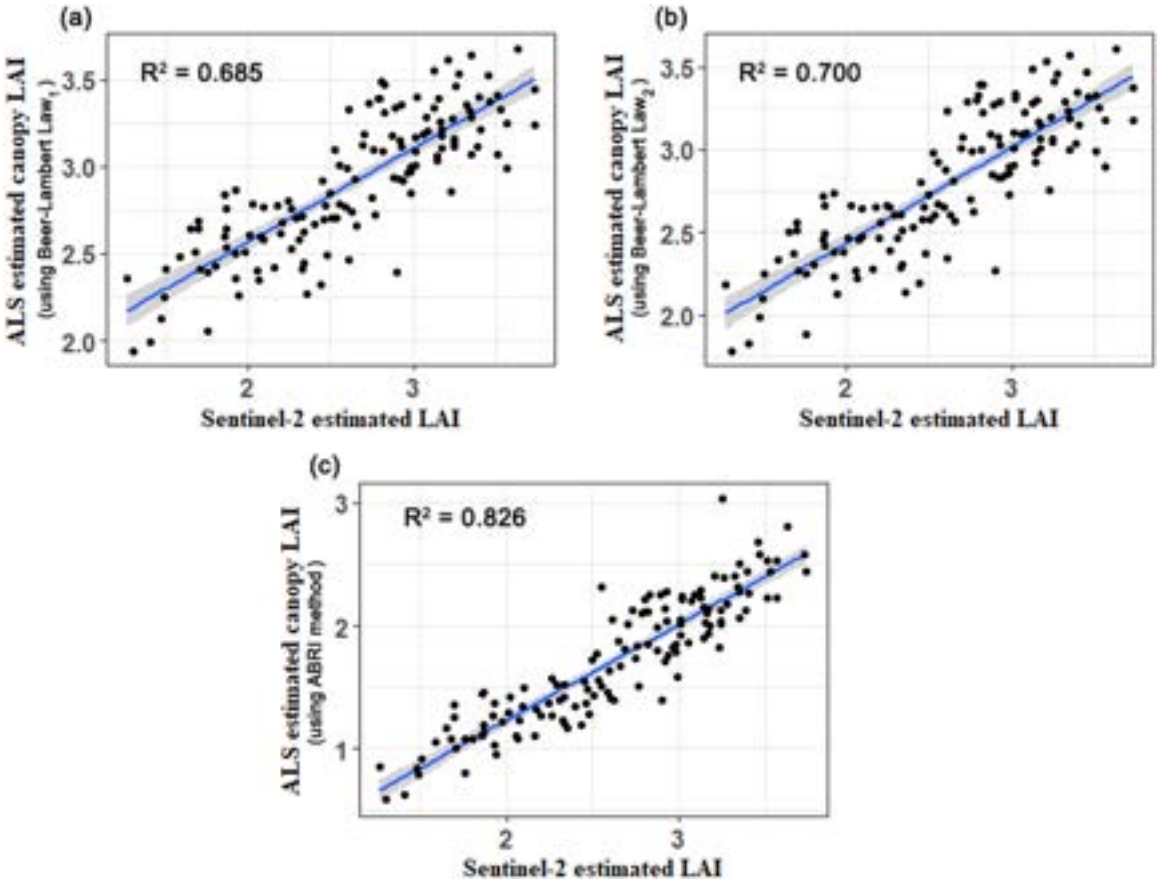

Fig. 7. Results of comparing three methods for estimating canopy leaf area index (LAI) using airborne laser scanning (ALS) against LAI estimated by Sentinel-2. Shown are linear relationships calculated between Sentinel-2 estimated LAI and ALS-estimated LAI from: (a) understory and overstory LAI combined using a Beer-Lambert method; (b) canopy LAI only from a Beer-Lambert method; and (c) canopy LAI using the Above and Below Ratio Index (ABRI) method. Total number of observations (each with an area of 1600 m^2) = 133.

Table 9
Results of Type III analysis of variance for LAI change from pre-fertilization (October 2020) to one growing season post-fertilization (October 2021). All p-values (in bold) suggest strong evidence of statistical significance. Sum sq. and mean sq. refer to the sum and mean square terms for each explanatory factor in the model, NumDF and DenDF refer to the degrees of freedom of the numerator and denominator terms (determined via Satterthwaite's method) for the resulting F statistic, F refers to the ratio of mean square for the model factor to mean square of residuals, and p-value refers to the one-tailed probability of the null hypothesis with the associated F statistic.

Term	*Sum sq.*	*Mean sq.*	*NumDF*	*df*	*F*	*p-value*
Variable rate factor	0.203	0.203	1	51.48	5.08	**0.028**
Average understory height	0.386	0.386	1	48.95	9.70	**0.003**
Nitrogen rate applied	0.749	0.250	3	53.41	6.27	**0.001**
Herbicide application	0.275	0.275	1	6.12	6.92	**0.038**
Variable rate factor × average understory height	0.248	0.248	1	54.32	6.23	**0.016**
Variable rate factor × Herbicide application	0.002	0.002	1	51.85	0.06	0.804
Variable rate factor × Nitrogen rate applied	0.256	0.085	3	53.20	2.14	0.106
Herbicide application × Nitrogen rate applied	0.046	0.015	3	53.23	0.39	0.763

through the canopy (e.g. LI-COR LAI2200, see Sumnall et al., 2021). As LiDAR acquisitions are themselves expensive and therefore less common, the relationship of ALS-derived metrics with satellite imagery allows for greater access to LAI time-series at a sub-stand level to assess stand productivity trajectories, as LAI can be a predictor of annual volume increment (Will et al., 2005). The relative level of correlation between ALS-derived canopy LAI with Sentinel-2 LAI was better than expected due to the known issues when the understory is evergreen (Peduzzi et al., 2010).

4.2. Variable-rate applications and analytical results

The calibration flight and variable-rate application operation results showed that accurate sub-stand level fertilizer application was both feasible and successful. We found strong evidence that LAI responded to fertilization one year post-treatment application and was potentially related to the total amount of N and P applied. Previous research has shown extensive nutrient deficiencies of N and P in the study region (Fox et al., 2007) and our results corroborate findings of early response to fertilization (*e.g.*, Albaugh et al., 2019; Pritchett and Swinford, 1961; Gent et al., 1986), but on a much larger scale than ever previously tested and reported.

Our results show that LAI can be estimated at midrotation following thinning using Sentinel-2 and be used to inform fertilizer rates according to LAI thresholds. These LAI-based N application led to detectable change in LAI that were potentially responsive to the applied nutrient addition rate. Our results further showed that fertilizer applications rates informed by remotely sensed LAI showed greater increases in LAI

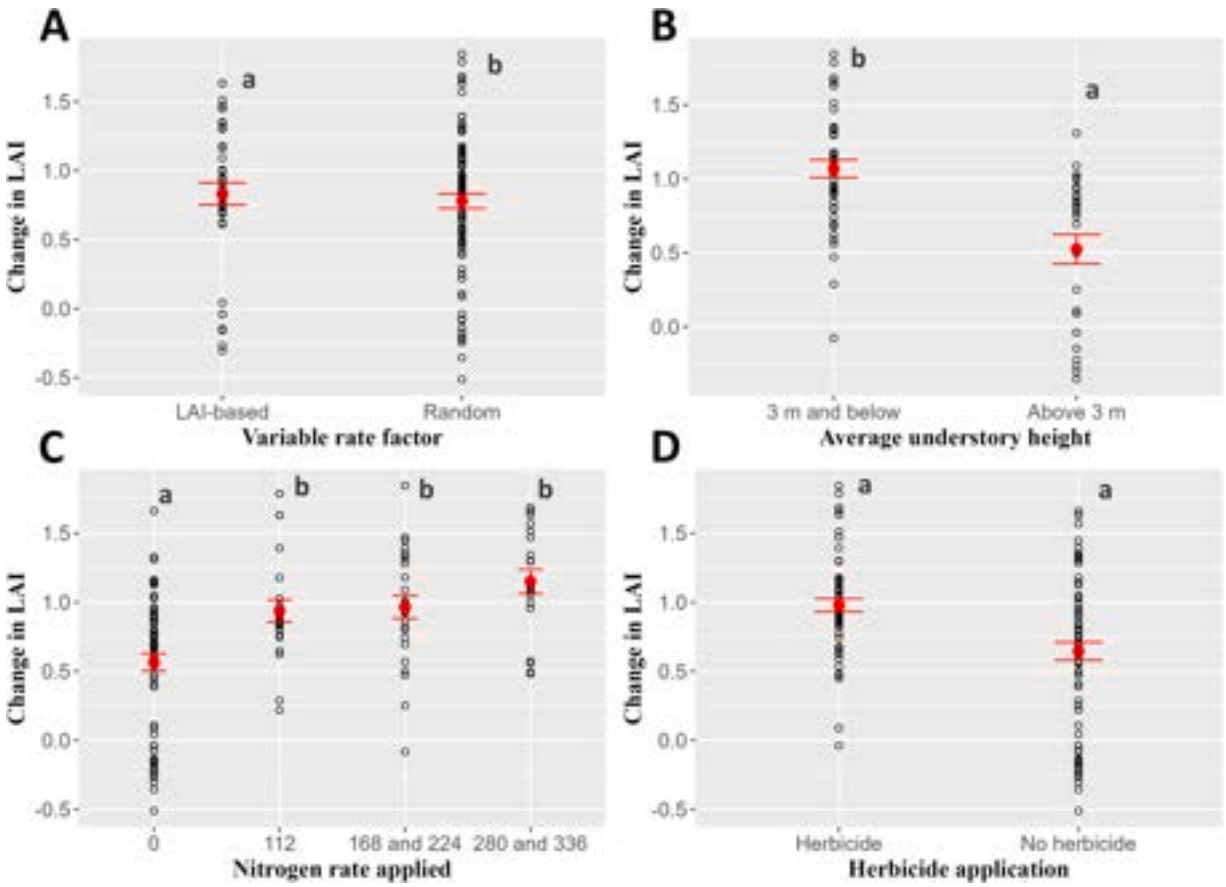

Fig. 8. LAI change from pre-fertilization (October 2020) to one growing season post-fertilization (October 2021), by experimental factors. Nitrogen rate applied (kg N ha^{-1}) was always applied with 10 % elemental P. Red points and error bars represent raw mean and standard error by factor. Letters designate significant marginal mean groupings of the linear mixed model for LAI change.

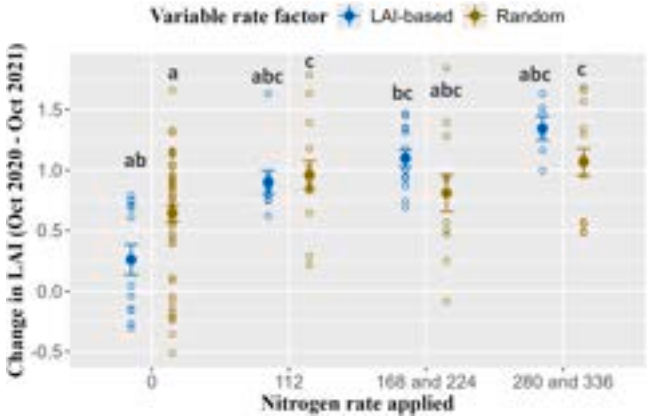

Fig. 9. LAI change from pre-fertilization (October 2020) to one growing season post-fertilization (October 2021), by N rate applied and variable rate factor. Nitrogen rate applied (kg N ha^{-1}) was always applied with 10 % elemental P. Filled points and error bars represent raw mean and standard error. Letters designate significant marginal mean groupings of the linear mixed model for LAI change, where higher letter values equate to higher marginal means. LAI-based rates of applied N are shown in blue and randomly applied rates of N are shown in mustard yellow. Nitrogen rate applied was always linked with elemental P respective of 10 % total applied elemental N.

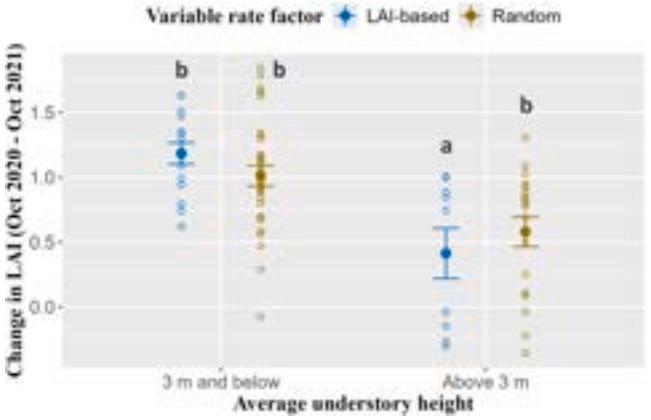

Fig. 10. LAI change from pre-fertilization (October 2020) to one growing season post-fertilization (October 2021), by understory height and variable rate factor. Filled points and error bars represent raw mean and standard error. Letters designate significant marginal mean groupings of the linear mixed model for LAI change, where higher letter values equate to higher marginal means. LAI-based rates of applied N are shown in blue and randomly applied rates of N are shown in mustard yellow.

than randomly assigned rates. More robust response in LAI gain with targeted LAI-based fertilizer N + P rates may be the product of more efficient targeting of larger quantities of nutrients to areas evincing greater nutrient deficiency (low starting LAI), leading to larger and more even LAI gains post-fertilization than randomly distributed fertilizer rates.

Strong evidence suggested that herbicide application was related to changes in crop tree canopy LAI, though mean differences were not significant and shifts in LAI were in some cases within the margin of

Table 10
Mean October LAI incremental change values from pre-fertilization (2020) and one growing season post-fertilization (2021), separated by individual stand and then subdivided by herbicide application status (herbicide application conducted in May 2020, one growing season prior to fertilization).

Stand ID	*Herb or No Herb*	*Mean October LAI incremental change*
North1	Herb	+ 0.54
	No Herb	- 0.01
North2	Herb	+ 0.96
	No Herb	+ 0.76
North3	Herb	+ 1.26
	No Herb	+ 0.90
South1	Herb	+ 1.28
	No Herb	+ 1.18
South2	Herb	+ 0.92
	No Herb	+ 0.68

Fig. 11. Map of stand "North1" depicting relative change in LAI following a variable-rate fertilizer application. Change in LAI is calculated as the difference between mean LAI of composite Sentinel-2 averages for quality-inspected acquisitions during the months of October, compared between the time period of 2021 and 2020. Fertilizer was applied in March 2021 with rates varying across 100 × 100 m spatial grids. Midrotation release was conducted via skidder-applied herbicide in May 2020, with sides contained by red boundary indicating region of herbicide application ("herb") and black boundary indicating no herbicide was applied ("no herb").

error for detection (0.4 units of LAI) when using Sentinel-2 estimated LAI. Lower mean understory height showed strong evidence of association with greater LAI change, possibly indicative of successful understory control where herbicides were applied. Our results appear to follow previous research that suggests fertilization has greater impact than midrotation release via herbicide, but that both contribute to crop tree growth (Albaugh et al., 2012). There was no relationship between understory height and prior herbicide application. We hypothesize a potential correlation between understory LAI removal and overstory LAI increase (Albaugh et al., 2013), though future LiDAR acquisitions will be necessary to quantify this relationship more accurately.

4.3. Future research directions

This study could be further enhanced by incorporating more stands across a wider study area, by examining a longer temporal window of analysis post-fertilization, and conducting additional analysis of ground-based inventory metrics (*e.g.*, heights, diameters, live crown length) as they relate to treatments over time. Because the duration of fertilizer effects is expected to increase with rate (up to 17 years, Albaugh et al., 2021), the long-term impacts of vegetation control and variable-rate fertilization in operational pine plantations have only just begun to be understood at this scale and at these test sites. Further analysis needs to be conducted regarding relative response in different soil and geologic

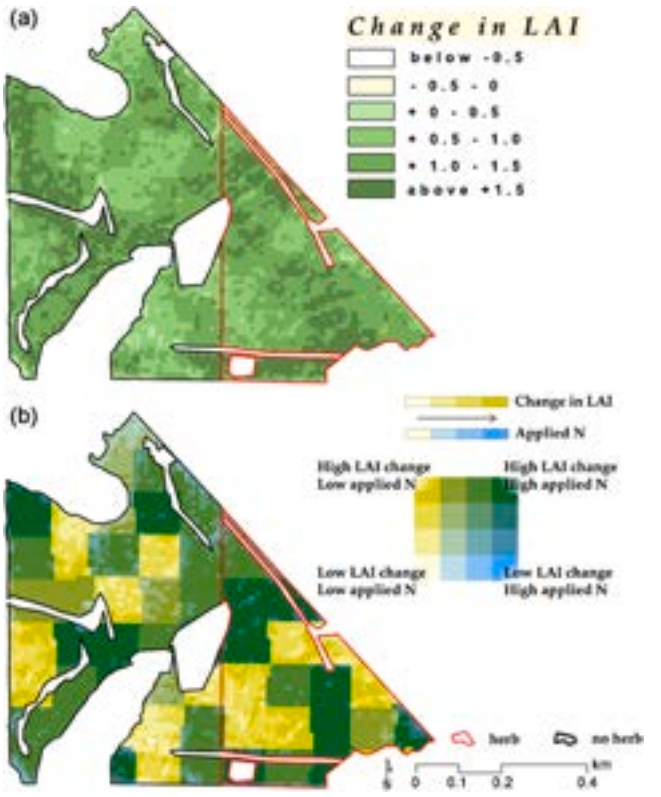

Fig. 12. Two maps visualizing post-variable-rate fertilization for stand "South1." Specifically displayed are: (a) relative change in LAI (Oct 2020 to Oct 2021); and (b) bivariate symbolization of change in LAI relative to applied N rate as was prescribed and varied on a 100 × 100 m treatment zone basis.

parent materials to tailor fertilizer regimes to include the appropriate nutrients where required.

We used single images from 30 September 2020 for each stand to establish baseline LAI values upon which to prescribe varying rates of fertilizer. This approach reflects the ordinary route for evaluating land cover with satellite imagery that was prevalent in the pre-cloud computing era (e.g. Sivanpillai et al., 2006). However, the advent of greater data handling capacity with cloud-based systems like Earth Engine has permitted a more intensive use of the image time-series data available. Exploring the time series of LAI for each stand and inspecting respective composites of monthly mean LAI for static locations leads us to believe the use of monthly average LAI rather than a single acquisition of LAI may improve similar works in the future. The exact time period in which LAI should be evaluated is dependent on the silvicultural objectives seeking to be accomplished, but it would be useful to focus future study on the ways satellite-derived LAI dynamics best reveal opportunities for silvicultural treatments—for instance, which seasons or seasonal patterns are most closely indicative of LAI and nutrient deficiency, and which are most associated with understory density.

Additional N and P availability can be deployed by the plant both toward producing more leaf tissue biomass and raising leaf tissue chlorophyll content, though in the case of Loblolly pine the accumulation of greater leaf biomass with fertilization seems to drive enhanced aboveground biomass growth (Albaugh et al., 1998; Vose and Allen, 1988). Tissue N content is positively correlated with chlorophyll content and also affects the reflectance signature of pine needles (Major and Mosseler, 2021; Tsay et al., 1982). The total amount and area of leaf biomass present, its arrangement in the space of the canopy volume, and the photosynthetic capacity of the leaf tissue per unit of biomass are all important determinants of the carbon assimilation potential of a forest stand. These factors also influence the reflectance signature of a given pine stand (Gholz et al., 1997). In this study we only examined estimated

LAI of the stand both as an indicator of starting nutrient status and the subsequent growth response of the stands following fertilization. This estimated LAI was itself a proxy estimate modeled based on the relative reflectance of the canopy in two spectral bands measured by Sentinel-2 (red and near-infrared) (Cohrs et al., 2020). Future research should delve further into teasing apart the several factors driving canopy reflectance to better understand the reflectance signatures of stand nutrient status and their indication of silvicultural response in managed pine of this type.

This study did not evaluate tree stem volume response, growth efficiency, or other metrics of value to the forest science community in relation to LAI. The analysis was prepared at an early stage in this longer-term field experiment, before extensive field measurements were available that could assess the growth of woody fractions as in other timber growth response experiments. Though prior work has shown a strong correlation between greater LAI and greater biomass growth with nutrient addition (Vose and Allen, 1988), woody biomass growth response could not be measured directly in this study. Future research, drawing on field data accumulated since this experimental site was installed, will help to fill in this gap. This study instead focused on assessing the use of remote sensing imagery to both plan and then evaluate precision silvicultural treatments at a field scale. Further exploration of understory dynamics in relation to herbicide application and fertilization would improve our understanding of the relationship between midrotation release treatments and fertilization. Recent advancements in understory quantification and mapping via ALS as well as passive radiometric sensors will require investigation to find relationships with field-collected annual understory metrics. Kriging-based interpolation methods or more flexible machine-learning approaches to estimate understory with respect to LAI and soil gradients throughout each study site could unlock potential for robust spatial statistical analyses.

One of the main draws of conducting precision silviculture as demonstrated in this experiment is the prospect for more economical use of costly inputs and interventions, targeting e.g. fertilizer and competition control to stands at the place and rate needed. Effective, semi-continuous monitoring of stand characteristics via remote sensing (satellite imagery and ALS point clouds) is an activating capability toward this shift in management strategy. On the other hand increasing complexity of sub-stand management and the technical expertise required to effectively use the relevant remotes sensing data streams, as well as the relative fluctuation in the costs of inputs and value of lumber product outputs, introduce additional complexity for the forest land manager in contemplating adoption of precision silvicultural practices (Fox et al., 2007). As growth and response data become available, more specific return on investment analysis from this study will be critical to assess the relative cost and benefit of herbicide and/or fertilizer treatments such as these tested at midrotation. More precise modeling of fertilizer and herbicide treatments, which can fluctuate greatly in cost, with remote sensing information will allow forest managers to make more informed decisions that ever before possible. Additional experimental experience in the methods for precision application of these inputs at variable rates, available application platforms and logistical concerns, and other factors such as existing feature like haul roads and thinning row placement, will need to be incorporated into the thinking of forest managers in treatment zone delineation. The process of transitioning from homogenous forest stand management to site-specific, precision grid-based forest management would likely be improved by utilizing a combination of metrics summarizing the site and its optimal treatment prescription. The use of remotely sensed LAI may also prove appropriate for a data fusion approach with other site variables like soil properties, which in agricultural contexts have shown potential for improving the understanding of the spatial variation occurring across potential management zones (Shaddad et al., 2016).

5. Conclusions

Technological advancements in fixed-wing aircraft fertilizer spreader technology have made fertilization application possible at smaller sub-stand spatial scales which, along with enabling advances in satellite and aerial remote sensing and GIS, are poised to permit forest managers to optimize nutrient management decisions based on freely available remote sensing data. Our findings lay the groundwork for the future of precision forestry management, exhibiting the potential for making better use of limited natural resources for managing a land basis that is projected to only get smaller in the future. Precision forestry in an operational loblolly pine plantation context was established by way of site-specific, grid-based delineation of five previously homogenously managed stands halfway through their typical rotation. We showed that LAI estimated via Sentinel-2 was strongly representative of canopy LAI estimates derived from contemporary ALS methods, and that thresholds can be created based on these LAI measurements to make better-informed decisions for fertilization rates. Reduced understory competition was associated with increased LAI one growing season post-fertilization, but the primary increases to LAI were related to the application of N + P. Future research should explore site-specific responses in tree volume linked to monitored LAI shifts over time, and the ways that soils, geology, site, and tree genetics may play a role in the growth and productivity of these southeastern US pine plantations.

CRediT authorship contribution statement

Rafael A. Rubilar: Supervision, Validation, Conceptualization, Writing – review & editing, Funding acquisition. **Otávio C. Campoe:** Writing – review & editing, Conceptualization, Supervision. **Andrew Trlica:** Writing – review & editing, Data curation, Formal analysis, Methodology. **Matthew Sumnall:** Data curation, Methodology, Writing – review & editing. **Simerjeet Virk:** Supervision, Writing – review & editing, Conceptualization, Methodology. **Mark V. Corrao:** Writing – review & editing, Conceptualization, Supervision. **Chris W. Cohrs:** Writing – review & editing, Project administration, Formal analysis, Software, Investigation, Conceptualization, Writing – original draft, Methodology, Data curation. **Rex Lester:** Resources, Investigation, Writing – review & editing, Methodology, Project administration, Conceptualization. **Al Lyons:** Resources, Writing – review & editing, Conceptualization, Project administration. **Rachel L. Cook:** Supervision, Methodology, Formal analysis, Writing – review & editing, Project administration, Funding acquisition, Resources, Investigation, Conceptualization. **David R. Carter:** Writing – review & editing, Project administration, Conceptualization, Resources, Funding acquisition, Supervision, Methodology. **Timothy J. Albaugh:** Resources, Conceptualization, Supervision, Data curation, Writing – review & editing, Project administration.

Declaration of Competing Interest

The authors declare that they have no known competing financial interests or personal relationships that could have appeared to influence the work reported in this paper.

Acknowledgements

We gratefully acknowledge the continued support of the Forest Productivity Cooperative. This work would not have been possible without the support of Manulife Investment Management. Other funding sources include NSF IUCRC Center for Advanced Forestry Systems (Award #1916552) and the program ANID BASAL (FB210015). We also receive support from the North Carolina State University Department of Forestry and Environmental Resources; Virginia Tech Department of Forest Resources and Environmental Conservation; the Facultad de Ciencias Forstales, Universidad de Concepción; and the Departamento

de Ciências Florestais, Universidade Federal de Lavras. Funding for this work was provided in part by the McIntire-Stennis Program of the National Institute of Food and Agriculture, U.S. Department of Agriculture Access No. 1025518. The use of trade names in this paper does not imply endorsement by the associated agencies of the products named nor criticism of similar ones not mentioned.

Appendix A

Table A1
Summary of pan catch for "112–1" grid during the variable-rate fertilization calibration flight that took place in Inverness, MS on 20 March 2021. The target application rate for this grid was 112 kg ha^{-1}

Pan #	*Pan location as on x-axis (m)*	*Pan collection mass (g)*	*App rate (kg ha^{-1})*
1	−12.2	0.745	123.2
2	−9.8	0.78	129.0
3	−7.3	0.687	113.6
4	−4.9	0.742	122.7
5	−2.4	0.72	119.0
C	0.0	0.62	102.5
6	2.4	0.675	111.6
7	4.9	0.808	133.6
8	7.3	0.75	124.0
9	9.8	0.857	141.7
10	12.2	0.963	159.2
		Mean	125.5
		Std. Dev.	15.5
		CV	13.8

Table A2
Summary of pan catch for "224" grid during the variable-rate fertilization calibration flight that took place in Inverness, MS on 20 March 2021. The target application rate for this grid was 224 kg ha^{-1}

Pan #	*Pan location as on x-axis (m)*	*Pan collection mass (g)*	*App rate (kg ha^{-1})*
1	−12.2	1.173	193.9
2	−9.8	1.250	206.7
3	−7.3	1.355	224.0
4	−4.9	1.443	238.6
5	−2.4	1.567	259.1
C	0.0	1.486	245.7
6	2.4	1.322	218.6
7	4.9	1.335	220.6
8	7.3	1.338	221.2
9	9.8	1.460	241.3
10	12.2	1.244	205.7
		Mean	225.0
		Std. Dev.	19.5
		CV	9.7

Table A3
Summary of pan catch for "168" grid during the variable-rate fertilization calibration flight that took place in Inverness, MS on 20 March 2021. The target application rate for this grid was 168 kg ha^{-1}

Pan #	*Pan location as on x-axis (m)*	*Pan collection mass (g)*	*App rate (kg ha^{-1})*
1	−12.2	1.089	180.0
2	−9.8	1.194	197.4
3	−7.3	1.090	180.2
4	−4.9	1.035	171.1
5	−2.4	1.093	180.7
C	0.0	1.041	172.1
6	2.4	0.998	165.0
7	4.9	1.066	176.2
8	7.3	1.038	171.6
9	9.8	0.918	151.8
10	12.2	0.894	147.8
		Mean	172.2
		Std. Dev.	13.8
		CV	9.7

Table A4
Summary of pan catch for "280" grid during the variable-rate fertilization calibration flight that took place in Inverness, MS on 20 March 2021. The target application rate for this grid was 280 kg ha^{-1}

Pan #	*Pan location as on x-axis (m)*	*Pan collection mass (g)*	*App rate (kg ha^{-1})*
1	−12.2	1.502	248.3
2	−9.8	1.693	279.9
3	−7.3	1.748	289.0
4	−4.9	1.815	300.1
5	−2.4	1.991	329.2
C	0.0	1.910	315.8
6	2.4	1.807	298.8
7	4.9	1.546	255.6
8	7.3	1.733	286.5
9	9.8	1.584	261.9
10	12.2	1.492	246.7
		Mean	282.9
		Std. Dev.	27.4
		CV	10.9

Table A5
Summary of pan catch for "336" grid during the variable-rate fertilization calibration flight that took place in Inverness, MS on 20 March 2021. The target application rate for this grid was 336 kg ha^{-1}

Pan #	*Pan location as on x-axis (m)*	*Pan collection mass (g)*	*App rate (kg ha^{-1})*
1	−12.2	1.713	283.2
2	−9.8	1.814	299.9
3	−7.3	2.122	350.8
4	−4.9	2.357	389.7
5	−2.4	2.388	394.8
C	0.0	2.161	357.3
6	2.4	2.008	332.0
7	4.9	2.284	377.6
8	7.3	2.141	354.0
9	9.8	1.872	309.5
10	12.2	1.721	284.5
		Mean	339.4
		Std. Dev.	40.5
		CV	13.4

Table A6
Summary of pan catch for "112–2" grid during the variable-rate fertilization calibration flight that took place in Inverness, MS on 20 March 2021. The target application rate for this grid was 112 kg ha^{-1}

Pan #	*Pan location as on x-axis (m)*	*Pan collection mass (g)*	*App rate (kg ha^{-1})*
1	−12.2	0.780	129.0
2	−9.8	0.768	127.0
3	−7.3	0.764	126.3
4	−4.9	0.804	132.9
5	−2.4	0.706	116.7
C	0.0	0.611	101.0
6	2.4	0.658	108.8
7	4.9	0.839	138.7
8	7.3	0.808	133.6
9	9.8	0.865	143.0
10	12.2	0.804	132.9
		Mean	126.4
		Std Dev.	12.7
		CV	11.3

Data availability

Data will be made available on request.

References

Albaugh, T.J., Allen, H.L., Dougherty, P.M., Kress, L.W., King, J.S., 1998. Leaf area and above- and belowground growth responses of Loblolly pine to nutrient and water additions. For. Sci. 44 (2), 317–328.

Albaugh, T.J., Stape, J.L., Fox, T.R., Rubilar, R.A., Allen, H.L., 2012. Mid-rotation vegetation control and fertilization response in *Pinus taeda* and *Pinus elliottii* across the southeastern United States. South. J. Appl. For. 36 (1), 44–53.

Albaugh, T.J., Fox, T.R., Blinn, C.E., Allen, H.L., Rubilar, R.A., Stape, J.L., 2013. Developing a new foliar nutrient-based method to predict response to competing vegetation control in *Pinus taeda.* South. J. Appl. For. 37 (4), 196–201.

Albaugh, T.J., Fox, T.R., Cook, R.L., Raymond, J.E., Rubilar, R.A., Campoe, O.C., 2019. Forest fertilizer applications in the southeastern United States from 1969 to 2016. For. Sci. 65 (3), 355–362.

Albaugh, T.J., Albaugh, J.M., Carter, D.M., Cook, R.L., Cohrs, C.W., Rubilar, R.A., Campoe, O.C., 2021. Duration of response to nitrogen and phosphorus applications in mid-rotation *Pinus taeda*. For. Ecol. Manag. 498, 119578.

Alig, R.J., Butler, B.J., 2004. Projecting large-scale area changes in land use and land cover for terrestrial carbon analyses. Environ. Manag. 33, 443–456.

Allen, H.L., 2001. Silvicultural treatments to enhance productivity. In: Evans, J. (Ed.), The Forests Handbook: Applying Forest Science for Sustainable Management, 2. Blackwell Science, Oxford, UK, pp. 129–139.

Allen, H.L., Kelting, D.L., Albaugh, T.J., 2001. Nutrient management concepts and practices in southern pine plantations. Enhanced forest management: fertilization and economics. Clear Lake Ltd., Edmonton, Canada, pp. 27–31.

Bahr, A., Ellström, M., Akselsson, C., Ekblad, A., Mikusinska, A., Wallander, H., 2013. Growth of ectomycorrhizal fungal mycelium along a Norway spruce forest nitrogen deposition gradient and its effect on nitrogen leakage. Soil Biol. Biochem. 59, 38–48.

Bates, D., Mächler, M., Bolker, B., Walker, S., 2015. Fitting linear mixed-effects models using lme4. J. Stat. Softw. 67 (1), 1–48.

Blinn, C.E., Albaugh, T.J., Fox, T.R., Wynne, R.H., Stape, J.L., Rubilar, R.A., Allen, H.L., 2012. A method for estimating deciduous competition in pine stands using Landsat. South. J. Appl. For. 36 (2), 71–78.

Cohrs, C.W., Cook, R.L., Gray, J.M., Albaugh, T.J., 2020. Sentinel-2 Leaf Area Index estimation for pine plantations in the southeastern United States. Remote Sens. 12 (9), 1406.

Copernicus Data Space Ecoystem. 2020. Sentinel-2 data, dataspace browser, ⟨https://browser.dataspace.copernicus.eu⟩ (1 December 2020), processed by ESA.

Fox, T.R., Allen, H.L., Albaugh, T.J., Rubilar, R., Carlson, C.A., 2007. Tree nutrition and forest fertilization of pine plantations in the southern United States. South. J. Appl. For. 31 (1), 5–11.

Fox, T.R., Miller, B.W., Rubilar, R., Stape, J.L., Albaugh, T.J., 2011. Phosphorus nutrition of forest plantations: the role of inorganic and organic phosphorus. In: Bünemann, E., Oberson, A., Frossard, E. (Eds.), Phosphorus in Action. Springer, Berlin, Heidelberg, pp. 317–338.

Franklin, S.E., Lavigne, M.B., Deuling, M.J., Wulder, M.A., Hunt Jr., E.R., 1997. Estimation of forest leaf area index using remote sensing and GIS data for modelling net primary production. Int. J. Remote Sens. 18, 3459–3471.

Gent Jr., J.A., Allen, H.L., Campbell, R.G., 1986. Phosphorus and nitrogen plus phosphorus fertilization in loblolly pine stands at establishment. South. J. Appl. For. 10 (2), 114–117.

Gholz, H.L., Curran, P.J., Kupiec, J.A., Smith, G.M., 1997. Assessing leaf area and canopy biochemistry of florida pine plantations using remote sensing. In: Shimoda, H., Gholz, H.L., Nakane, K. (Eds.), The Use of Remote Sensing in the Modeling of Forest Productivity. Forestry Sciences, Vo. 50. Springer, Dordrecht.

Gorelick, N., Hancher, M., Dixon, M., Ilyushchenko, S., Thau, D., Moore, R., 2017. Google Earth Engine: Planetary-scale geospatial analysis for everyone. Remote Sens. Environ. 202, 18–27.

Guo, J., Prestemon, J., Johnston, C., 2023. Forest market outlook in the southern United States. For. Policy Econ. 157, 103091.

Hothorn, T., Bretz, F., Westfall, P., 2008. Simultaneous inference in general parametric models. Biom. J. 50 (3), 346–363.

Lenth, R. 2025. *emmeans*: Estimated marginal means, aka least-squares means. R package version 1.10.7-100001. ⟨https://rvlenth.github.io/emmmeans⟩.

Lowenberg-DeBoer, J., Erickson, B., 2019. Setting the record straight on precision agriculture adoption. Agron. J. 111 (4), 1152–1569.

Lüdecke, D., Ben Shachar, M., Patil, I., Waggoner, P., Makowski, D., 2021. *performance*: An R package for assessment, comparison and testing of statistical models. J. Open Source Softw. 6 (60), 3139.

Major, J.E., Mosseler, A., 2021. Chlorophyll pigment and needle macronutrient response and interactions to soil moisture and atmospheric CO_2 treatments of eight pine and spruce species. Trees 35, 2069–2085.

Muff, S., Nilsen, E.B., O'Hara, R.B., Nater, C.R., 2022. Rewriting results sections in the language of evidence. Trends Ecol. Evol. 37 (3), 203–210.

Oswalt, S.N., Smith, W.B., Miles, P.D., Pugh, S.A., 2019. Forest Resources of the United States, 2017: A Technical Document Supporting the Forest Service 2020 RPA Assessment. U.S. Department of Agriculture, Forest Service, Washington, DC.

Payn, T., Carnus, J.-M., Freer-Smith, P., Kimberley, M., Kollert, W., Liu, S., Orazio, C., Rodriguez, L., Neves Silva, L., Wingfield, M.J., 2015. Changes in planted forests and future global implications. For. Ecol. Manag. 352, 57–67.

Peduzzi, A., Allen, H.L., Wynne, R.H., 2010. Leaf area of overstory and understory in pine plantations in the flatwoods. South. J. Appl. For. 34 (4), 154–160.

Pritchett, W.L., Swinford, K.R., 1961. Response of slash pine to colloidal phosphate fertilization. Soil Sci. Soc. Am. J. 25 (5), 397–400.

R Core Team, 2022. R: A Language Environment for Statistical Computing. R Foundation for Statistical Computing, Vienna, Austria. ⟨https://www.R-project.org⟩.

Salomonson, V.V., Appel, I., 2004. Estimating fractional snow cover from MODIS using the normalized difference snow index. Remote Sens. Environ. 89 (3), 351–360.

Shaddad, S.M., Madrau, S., Castrignanò, A., Mouazen, A.M., 2016. Data fusion techniques for delineation of site-specific management zones in a field in UK. Precis. Agric. 17 (2), 200–217.

Sivanpillai, R., Smith, C.T., Srinivasan, R., Messina, M.G., 2006. Estimation of managed loblolly pine stand age and density with Landsat ETM+ data. For. Ecol. Manag. 223 (1–3), 247–254.

Srinivasan, A., 2006. Precision agriculture: an overview. In: Srinivasan, A. (Ed.), Handbook of Precision Agriculture: Principles and Applications. Haworth Press, Inc, Binghamton, NY, pp. 1–16.

Subedi, S., Fox, T.R., Wynne, R.H., 2015. Determination of fertility rating (FR) in the 3-PG model for loblolly pine plantations in the Southeastern United States based on site index. Forests 6 (9), 3002–3027.

Sumnall, M., Peduzzi, A., Fox, T.R., Wynne, R.H., Thomas, V.A., Cook, B., 2016. Assessing the transferability of statistical predictive models for leaf area index between two airborne discrete return LiDAR sensor designs within multiple intensely managed Loblolly pine forest locations in the south-eastern USA. Remote Sens. Environ. 176, 308–319.

Sumnall, M.J., Trlica, A., Carter, D.R., Cook, R.L., Schulte, M.L., Campoe, O.C., Rubilar, R.A., Wynne, R.H., Thomas, V.A., 2021. Estimating the overstory and understory vertical extents and their leaf area index in intensively managed loblolly pine (*Pinus taeda* L.) plantations using airborne laser scanning. Remote Sens. Environ. 254, 112250.

Tsay, M.-L., Gjerstad, D.H., Glover, G.R., 1982. Tree leaf reflectance: a promising technique to rapidly determine nitrogen and chlorophyll content. Can. J. For. Res. 12 (4), 788–792.

Vose, J.M., Allen, H.L., 1988. Leaf area, stemwood growth, and nutrition relationships in loblolly pine. For. Sci. 34 (3), 547–563.

Wade, C.M., Baker, J.S., Latta, G., Ohrel, S.B., Allpress, J., 2019. Projecting the spatial distribution of possible planted forest expansion in the United States. J. For. 117 (6), 560–578.

Southern forest resource assessment. In: Wear, D.N., Greis, J.G., Wear, D.N., Greis, J.G. (Eds.), 2002. Gen. Tech. Rep. SRS-53. U.S. Department of Agriculture, Forest Service, Southern Research Station, Asheville, NC.

Will, R.E., Narahari, N.V., Shiver, B.D., Teskey, R.O., 2005. Effects of planting density on canopy dynamics and stem growth for intensively managed loblolly pine stands. For. Ecol. Manag. 205 (1–3), 29–41.

Zupanc, A. Improving Cloud Detection with Machine Learning. 2019. Available online: ⟨https://medium.com/sentinel-hub/improving-cloud-detection-with-machine-learning-c09dc5d7cf13⟩ (Accessed on 29 November 2019).